Interpolation of the coupling-ray-theory Green function within ray cells

Luděk Klimeš & Petr Bulant*
Department of Geophysics, Faculty of Mathematics and Physics, Charles University, Ke Karlovu 3, 121 16 Praha 2, Czech Republic, http://sw3d.cz

Abstract

The coupling–ray–theory tensor Green function for elastic S waves is frequency dependent, and is usually calculated for many frequencies. This frequency dependence represents no problem for calculating the Green function, but may be impractical or even unrealistic in storing the Green function at the nodes of dense grids, typical for applications such as Born approximation or non–linear source determination.

We have already proposed the approximation of the coupling–ray–theory tensor Green function, in the vicinity of a given prevailing frequency, by two coupling–ray–theory dyadic Green functions described by their coupling–ray–theory travel times and their coupling–ray–theory amplitudes.

The above mentioned prevailing–frequency approximation of the coupling ray theory enables us to interpolate the coupling–ray–theory dyadic Green functions within ray cells, and to calculate them at the nodes of dense grids. For the interpolation within ray cells, we need to separate the pairs of the prevailing–frequency coupling–ray–theory dyadic Green functions so that both the first Green function and the second Green function are continuous along rays and within ray cells. In this contribution, we describe the current progress in this field and outline the basic algorithms. We also demonstrate the preliminary numerical results in several velocity models.

Introduction

In sufficiently smooth media, the anisotropic ray theory (Babich, 1956; Červený, 2001) can be used to calculate elastic P waves at all degrees of anisotropy, including isotropic media. However, neither the isotropic ray theory (Luneburg, 1944; Babich, 1961; Červený, 2001) nor the anisotropic ray theory is applicable to calculating elastic S waves in many cases of heterogeneous anisotropic media. We should use the coupling ray theory proposed, e.g., by Kravtsov (1968) or by Coates & Chapman (1990) for elastic S waves.

Unfortunately, the coupling–ray–theory tensor Green function is frequency–dependent, and is calculated separately for each frequency. This frequency dependence represents the main obstacle for the interpolation of the coupling–ray–theory tensor Green function within ray cells.

Klimeš & Bulant (2016) found the approximation of the coupling–ray–theory tensor Green function in the vicinity of a given prevailing frequency by two prevailing–frequency coupling–ray–theory dyadic Green functions corresponding to two elementary coupling–ray–theory waves. Each prevailing–frequency coupling–ray–theory dyadic Green function is described by its coupling–ray–theory travel time and its complex–valued coupling–ray–theory amplitude tensor, both calculated for the given prevailing frequency. Klimeš & Bulant (2016) numerically demonstrated that the prevailing–frequency coupling–ray–theory dyadic Green functions are well applicable in a reasonably broad frequency band around the given prevailing frequency. The prevailing–frequency coupling–ray–theory dyadic Green functions are calculated along the reference rays, which may be represented, e.g., by the isotropic common reference rays, the anisotropic common reference rays, the anisotropic–ray–theory rays, or the SH and SV reference rays (Klimeš & Bulant, 2014). For the sake of conciseness, we shall refer hereinafter to the reference rays as the rays.

Method

Each ray corresponds to two ray parameters and is represented by a point in the ray–parameter domain. The ray–parameter domain is triangulated according to Bulant (1996), see Figure 10. The vertices of the triangles correspond to rays. Each triangle corresponds to a ray tube, and its three vertices correspond to three rays which form the edges of the ray tube. Each ray tube is sliced into ray cells according to Bulant & Klimeš (1999).

At each point of each ray, we have two prevailing–frequency coupling–ray–theory dyadic Green functions described by their coupling–ray–theory travel times and their coupling–ray–theory amplitude tensors. We wish to interpolate them within ray cells using the algorithm designed by Bulant & Klimeš (1999). For the interpolation within ray cells, we need to separate the pairs of the prevailing–frequency coupling–ray–theory dyadic Green functions so that both the first Green function and the second Green function are continuous along rays and within ray cells.

In this contribution, we implement the separation in two steps: In the first step, we copy each old ray to a pair of identical new rays and match the pair of the prevailing–frequency coupling–ray–theory dyadic Green functions with the pair of new rays so that each Green function is continuous along the corresponding new ray. As a result, each of the three edges of each ray tube is represented

by two new rays instead of one ray. In the second step, we double each ray tube and match the three pairs of new edge rays with the pair of ray tubes so that the Green function is continuous within either of the two ray tubes. For details on the continuity of the Green functions along the rays and within ray tubes refer to Klimeš & Bulant (2013).

Examples

We numerically test the interpolation of the coupling–ray–theory dyadic Green functions within ray cells using the elastic S waves. Following Pšenčík, Farra & Tessmer (2012) and Klimeš & Bulant (2016), we consider eight anisotropic velocity models referred to as QIH, QI, QI2, QI4, KISS, SC1 I, SC1 II and ORT. All these velocity models are laterally homogeneous. The density–reduced elastic moduli are linear functions of depth in all these velocity models. The density is constant.

For a sketch of the source–receiver configuration refer to Figure 1. We plot the relative coupling–ray–theory travel–time difference (half relative coupling–ray–theory travel–time splitting) in the vertical rectangular section bounded by the point source from the left, and by the vertical well from the right. The distance of the vertical well with receivers from the source is 1 km. The vertical extent of the rectangular section corresponds to the length of the vertical receiver profile considered by Klimeš & Bulant (2016) for the calculation of the coupling–ray–theory seismograms: QIH, QI, QI2, QI4 and KISS 0.6 km; SC1_I and SC1_II 1.4 km; ORT 1.6 km.

Velocity model QI is approximately transversely isotropic. Its reference symmetry axis is horizontal and forms a 45° angle with the source–receiver vertical plane. Velocity models QIH, QI2 and QI4 are derived from velocity model QI and mutually differ by their degrees of anisotropy. The differences of the elastic moduli in velocity models QIH, QI, QI2 and QI4 from the elastic moduli in the reference isotropic velocity model are determined by ratio 0.5:1:2:4. For the elastic moduli in velocity models QI, QI2 and QI4 refer to Bulant & Klimeš (2008). The relative coupling–ray–theory travel–time difference in the vertical source–receiver section in velocity models QIH, QI, QI2 and QI4 is displayed in Figures 2–5. Since the colour scale in each figure corresponds to the degree of anisotropy, the changes between Figures 2–5 illustrate different development of S–wave coupling and splitting in dependence on anisotropy, which was discussed by Červený, Klimeš & Pšenčík, 2007, fig. 21. Figures 2–5 would be practically identical and close to Figure 5 for anisotropic–ray–theory travel times.

Velocity model KISS represents velocity model QI described above, rotated by −44° about the vertical axis in order to position the reference symmetry axis, corresponding to the kiss S–wave singularity, just 1° from the source–receiver plane. The relative coupling–ray–theory travel–time difference in the vertical source–receiver section is displayed in Figure 6. Figures 3 and 6 thus represent two different vertical sections in the same velocity model.

Velocity model SC1_I is approximately transversely isotropic and its reference symmetry axis is horizontal. Its slowness surface contains a split intersection singularity, whereas velocity models QIH, QI, QI2 and QI4 display no exact nor split intersection singularity. The relative coupling–ray–theory travel–time difference in the vertical source–receiver section is displayed in Figure 7.

Velocity model SC1_II is analogous to SC1_I, but its reference axis of symmetry is tilted. The split intersection singularity in velocity model SC1_II is thus positioned differently in comparison with velocity model SC1_I. In the source–receiver plane, the split intersection singularity is close to horizontal slowness vectors. The relative coupling–ray–theory travel–time difference in the vertical source–receiver section is displayed in Figure 8.

In the orthorhombic velocity model ORT, the slowness surface contains four conical singularities. The rays leading from the source to the middle part of the receiver profile pass close to one of these singularities. This conical singularity then acts as an interface and smoothly but very rapidly converts the actual elastic S–wave polarization from the approximately anisotropic–ray–theory polarization S1 to the approximately anisotropic–ray–theory polarization S2, and vice versa. That is probably why the ray tubes in the vicinity of the conical singularity in velocity model ORT cannot be split into the pairs of tubes with continuous prevailing–frequency coupling–ray–theory dyadic Green functions. The relative coupling–ray–theory travel–time difference in the vertical source–receiver section is displayed in Figure 9. The diagonal grey zone corresponds to the ray tubes which cannot be split into the pairs of tubes with continuous prevailing–frequency coupling–ray–theory dyadic Green functions. The ray tubes in the ray–parameter domain in velocity model ORT are displayed in Figure 10. We can observe the regions around three of four conical singularities where the ray tubes cannot be split into the pairs of tubes with continuous prevailing–frequency coupling–ray–theory dyadic Green functions. The bottom–right region corresponds to the diagonal grey zone in Figure 9.

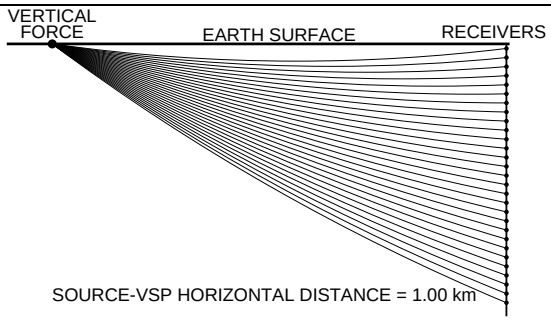

Figure 1: The source–receiver configuration for the calculationof the S-wave travel times, with a sketch of the rays leading to the receivers. The source is located at the Earth's surface, the receivers are placed in the vertical well. The depths of the receiver profiles are presented in the figures with travel-time differences.

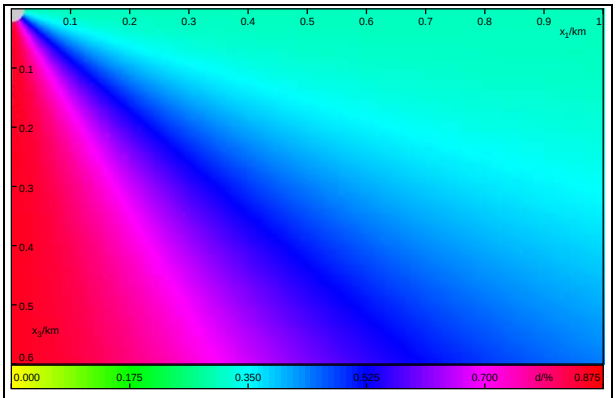

Figure 2: Relative coupling–ray–theory travel–time difference d in velocity model QIH.

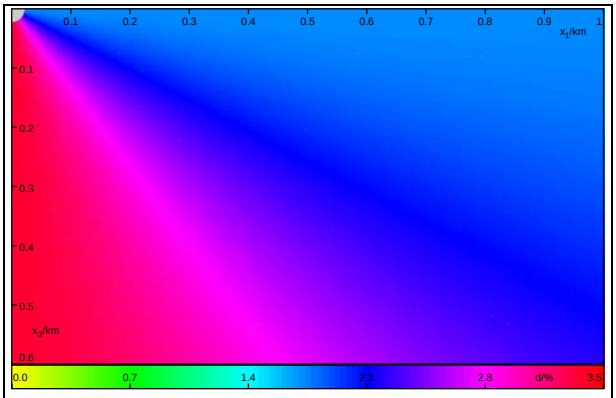

Figure 4: Relative coupling–ray–theory travel–time difference d in velocity model QI2.

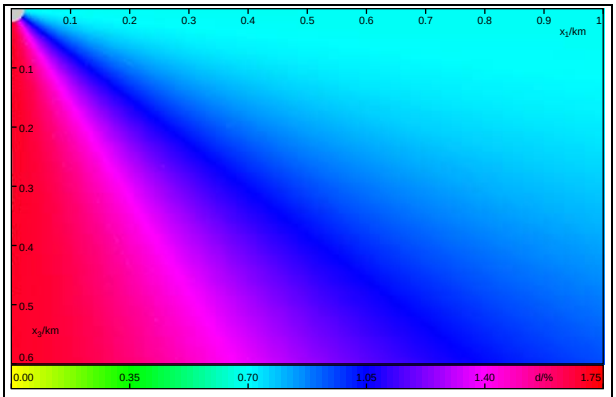

Figure 3: Relative coupling–ray–theory travel–time difference d in velocity model QI.

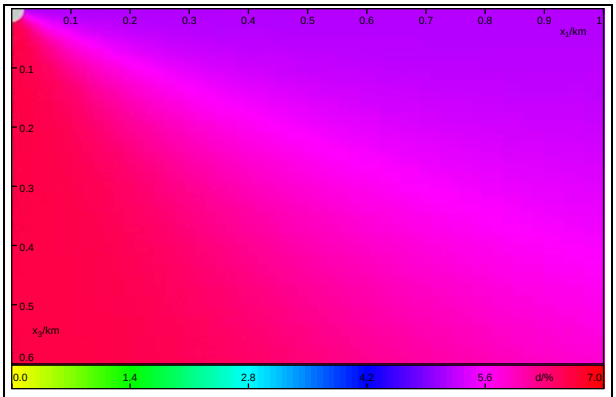

Figure 5: Relative coupling–ray–theory travel–time difference d in velocity model QI4. Since the colour scale in Figures 2–5 corresponds to the degree of anisotropy, the changes between the figures illustrate different development of S–wave coupling and splitting in dependence on anisotropy.

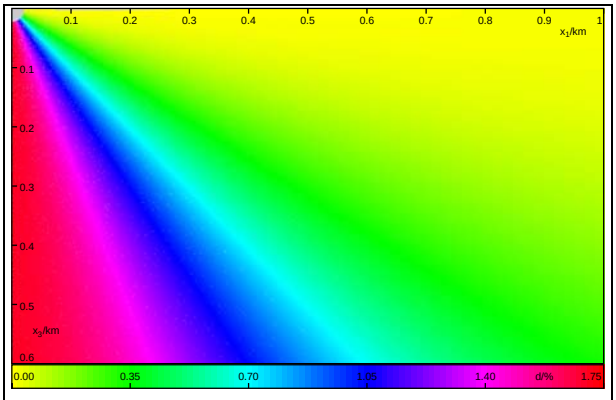

Figure 6: Relative coupling–ray–theory travel–time difference d in velocity model KISS. Velocity model KISS represents velocity model QI described above, rotated by −44° about the vertical axis, Figures 3 and 6 thus represent two different vertical sections in the same velocity model.

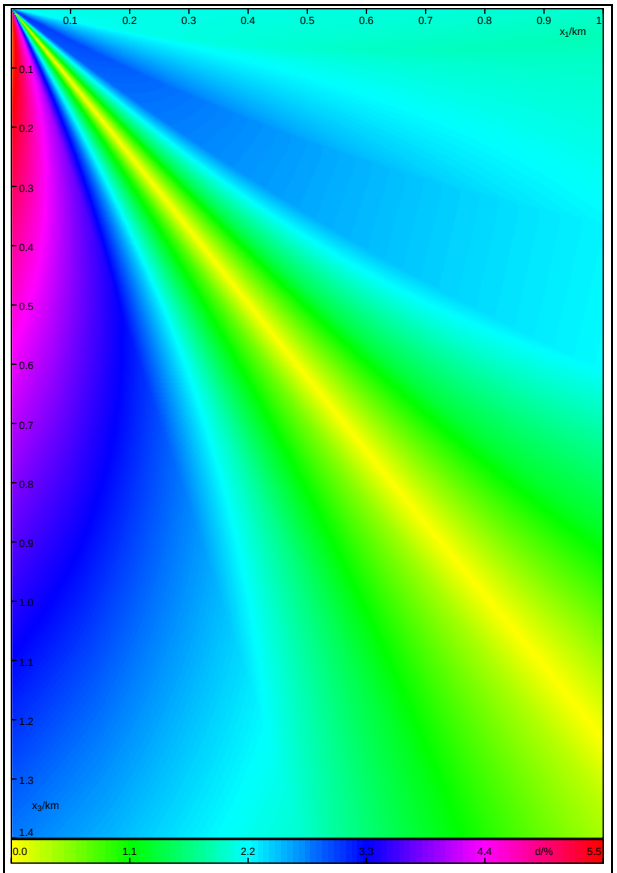

Figure 7: Relative coupling–ray–theory travel–time difference d in velocity model SC1_I.

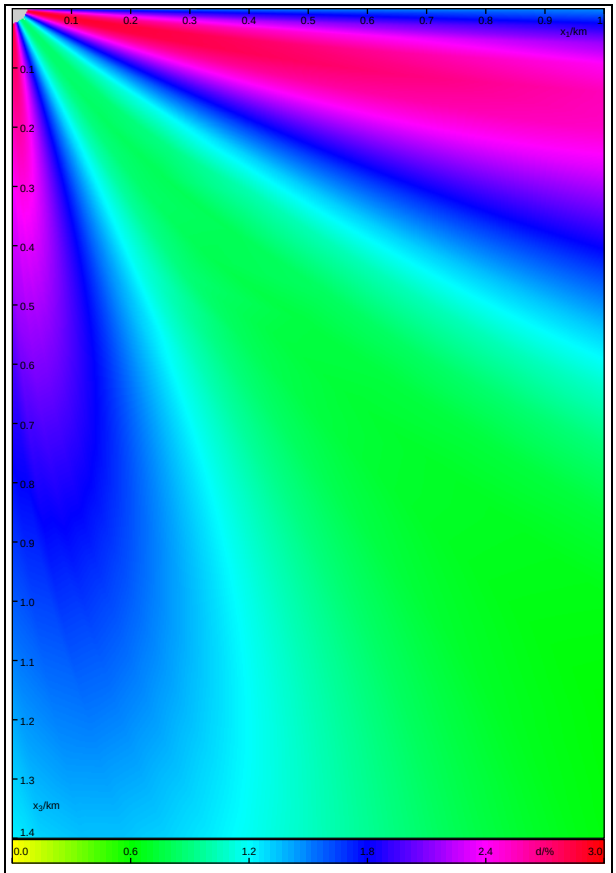

Figure 8: Relative coupling–ray–theory travel–time difference d in velocity model SC1_II.

Conclusions

The prevailing–frequency approximation of the coupling ray theory allows us to process the coupling–ray–theory wave field in terms of travel times and amplitudes, i.e., in the same way as the anisotropic–ray–theory wave field. The prevailing–frequency approximation of the coupling ray theory can thus be included in wavefront tracing and in the interpolation within ray cells in anisotropic media, provided that we can separate the pairs of the prevailing–frequency coupling–ray–theory dyadic Green functions so that both the first Green function and the second Green function are continuous within ray cells. In this contribution, we showed the preliminary version of the separation algorithm using eight numerical examples.

In the proposed preliminary version of the separation algorithm, the interpolation is possible only in ray tubes in which the prevailing–frequency coupling–ray–theory dyadic Green functions are continuous. This requirement may result in ray tubes where we cannot interpolate, like in Figure 9 in velocity model ORT. In order to refine the algorithm and extend the region where we can interpolate, we probably should study the continuity of the prevailing–frequency coupling–ray–theory dyadic Green functions in individual ray cells rather than in whole ray tubes.

Acknowledgments

The research has been supported by the Grant Agency of the Czech Republic under contracts 16-01312S and 16-05237S, by the Ministry of Education, Youth and Sports of the Czech Republic within research project CzechGeo/EPOS LM2015079, and by the members of the consortium “Seismic Waves in Complex 3–D Structures” (see “http://sw3d.cz”).

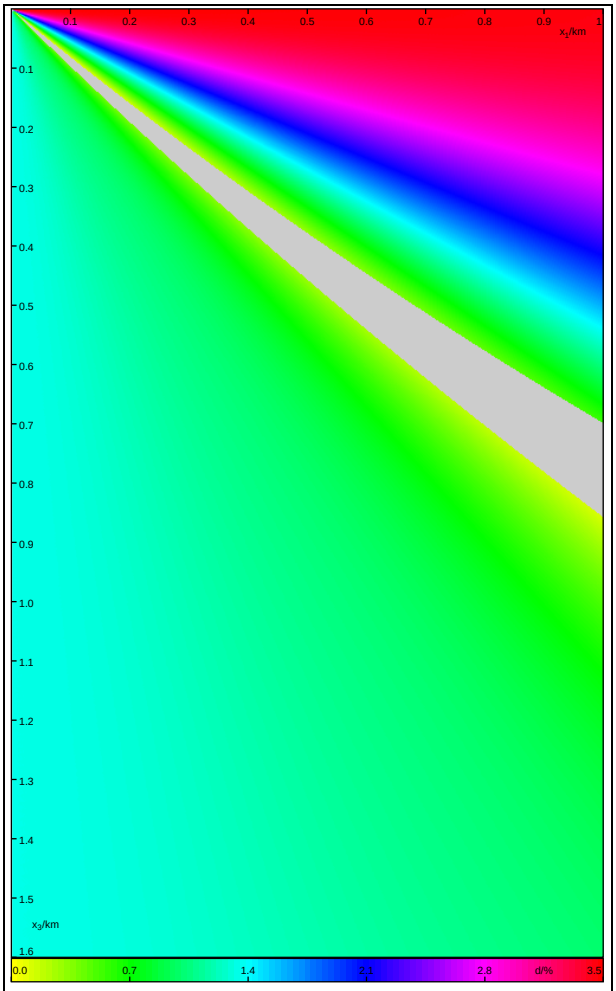

Figure 9: Relative coupling–ray–theory travel–time difference d in velocity model ORT. The rays leading from the source to the middle part of the receiver profile pass close to one of the conical singularities present in the model. This conical singularity then acts as an interface and smoothly but very rapidly converts the actual elastic S–wave polarization from the approximately anisotropic–ray–theory polarization S1 to the approximately anisotropic–ray–theory polarization S2, and vice versa. That is probably why the ray tubes in the vicinity of the conical singularity cannot be split into the pairs of tubes with continuous prevailing–frequency coupling–ray–theory dyadic Green functions, and the travel times thus can not be interpolated, forming the diagonal gray zone in the figure.

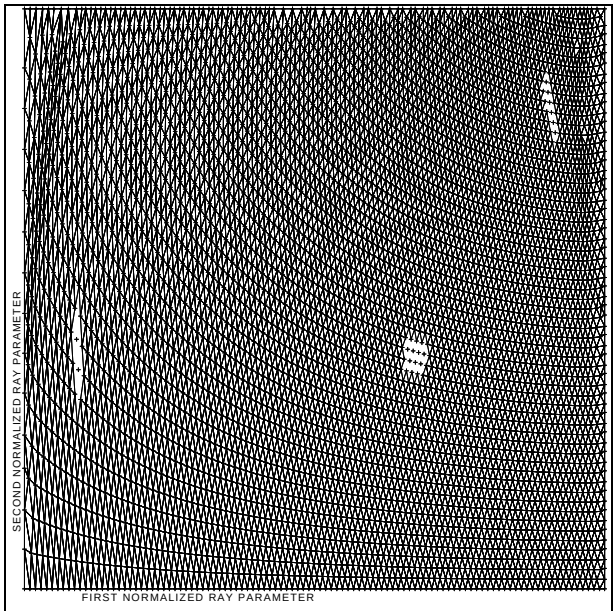

Figure 10: Ray tubes in velocity model ORT for the interpolation of coupling–ray–theory travel times. The rays are represented by points (here crosses) and the ray tubes by triangles in the ray–parameter domain. The three regions with missing triangles (ray tubes) are situated around the conical singularities where the ray tubes cannot be split into the pairs of tubes with continuous prevailing–frequency coupling–ray–theory dyadic Green functions. The bottom–right region corresponds to the diagonal grey zone in Figure 9.

References

Babich, V.M. (1956): Ray Method of the Computation of the Intensity of Wavefronts (in Russian). Doklady Akad. Nauk SSSR, 110, 355–357.

Babich, V.M. (1961): Ray method of calculating the intensity of wavefronts in the case of a heterogeneous, anisotropic, elastic medium (in Russian). In: Petrashen, G.I. (ed.): Problems of the Dynamic Theory of Propagation of Seismic Waves, Vol. 5, pp. 36–46, Leningrad Univ. Press, Leningrad, English translation: Geophys. J. int., 118(1994), 379–383.

Bulant, P. (1996): Two–point ray tracing in 3–D. Pure appl. Geophys., 148, 421–447.

Bulant, P. & Klimeš, L. (1999): Interpolation of ray theory traveltimes within ray cells. Geophys. J. int., 139, 273–282.

Bulant, P. & Klimeš, L. (2008): Numerical comparison of the isotropic–common–ray and anisotropic–common–ray approximations of the coupling ray theory. Geophys. J. int., 175, 357–374.

Červený, V. (2001): Seismic Ray Theory. Cambridge Univ. Press, Cambridge.

Červený, V., Klimeš, L. & Pšenčík, I. (2007): Seismic ray method: Recent developments. Advances Geophys., 48, 1–126.

Coates, R.T. & Chapman, C.H. (1990): Quasi–shear wave coupling in weakly anisotropic 3-D media. Geophys. J. int., 103, 301–320.

Klimeš, L. & Bulant, P. (2013): Interpolation of the coupling-ray-theory S-wave Green tensor within ray cells. Seismic Waves in Complex 3-D Structures, 23, 203-218, online at “http://sw3d.cz”.

Klimeš, L. & Bulant, P. (2014): Prevailing–frequency approximation of the coupling ray theory for S waves along the SH and SV reference rays in a transversely isotropic medium. Seismic Waves in Complex 3–D Structures, 24, 165–177, online at “http://sw3d.cz”.

Klimeš, L. & Bulant, P. (2016): Prevailing-frequency approximation of the coupling ray theory for electromagnetic waves or elastic S waves. Stud. Geophys. Geod., 60, 419–450, DOI: 10.1007/s11200-014-1070-4

Kravtsov, Yu.A. (1968): “Quasiisotropic” approximation to geometrical optics (in Russian). Dokl. Acad. Nauk SSSR, 183, 74–76, English translation: Sov. Phys. — Doklady, 13(1969), 1125–1127.

Luneburg, R.K. (1944): Mathematical Theory of Optics. Lecture notes, Brown University, Providence, Rhode Island, Reedition: University of California Press, Berkeley and Los Angeles, 1964.

Pšenčík, I., Farra, V. & Tessmer, E. (2012): Comparison of the FORT approximation of the coupling ray theory with the Fourier pseudospectral method. Stud. geophys. geod., 56, 35–64.